2684 *Macromolecules* **2010**, *43*, 2684–2691
DOI: 10.1021/ma100291z

Macromolecules
ARTICLE

Sulfonated Poly(arylene ether sulfone ketone) Multiblock Copolymers with Highly Sulfonated Block. Synthesis and Properties

Byungchan Bae,[†] Kenji Miyatake,*[,†,‡] and Masahiro Watanabe*[,†]

[†]*Fuel Cell Nanomaterials Center and* [‡]*Clean Energy Research Center, University of Yamanashi, 4 Takeda, Kofu 400-8510, Japan*

Received February 5, 2010

ABSTRACT: Poly(arylene ether sulfone ketone) (SPESK) multiblock copolymer membranes having highly sulfonated hydrophilic blocks were synthesized. The degree of polymerization of hydrophobic blocks (*X*) was controlled to be 15, 30, and 60 and that of hydrophilic blocks (*Y*) to be 4, 8, 12, and 16. Morphological observation by scanning transmission microscopy (STEM) and small-angle X-ray scattering (SAXS) showed that high local concentration of sulfonic acid groups within the hydrophilic blocks enhanced phase separation between the hydrophobic and hydrophilic blocks. Rodlike hydrophilic aggregates were found to be interconnected very well, which resulted in high proton conductivity even at low relative humidity (RH). The ionomer membrane with *X*30*Y*8 and 1.86 mequiv/g of ion exchange capacity (IEC) showed 0.03 S/cm at 80 °C and 40% RH, which was a comparable or higher proton conductivity than that of the state-of-the-art perfluorinated ionomer (Nafion) membrane. The longer blocks induced higher proton conductivity; however, excessively long block length offset mechanical properties. Low hydrogen and oxygen permeability was also observed.

Introduction

There have been great demands for clean energy or renewable energy sources in the past decade. The polymer electrolyte membrane fuel cell (PEMFC) has received considerable attention due to its high energy efficiency and lack of carbon dioxide emission. Perfluorosulfonic acid (PFSA) polymers such as Nafion (DuPont) are the most promising and state-of-the-art as polymer electrolyte membranes for PEMFC. However, some drawbacks such as high production cost, poor thermomechanical properties above 80 °C, and environmental inadaptability have been reported.[1−3] Aromatic hydrocarbon ionomers have been studied as alternative membranes, which include sulfonated poly(arylene ether sulfone)s (SPES),[4,5] poly(arylene ether ether ketone)s (SPEEK),[6−8] poly(arylene sulfide sulfone)s (SPSS),[9,10] polyimides (SPI),[11,12] poly(arylene ether nitrile)s,[13] polybenzimidazoles,[14,15] and polyphenylenes.[16,17] High proton conductivities were claimed for some of these polymers; however, proton conductivity at low hydration level (or low relative humidity (RH)) remains an issue. Performance of membranes at low RH and high temperature is critical for the practical applications to the PEMFC since it determines fuel cell performance and size of BOP (balance of plant) within the system.[18]

Proton conductivity of polymer electrolyte membranes is closely related to several parameters such as acidity, number and position of ionic groups, main chain and/or side chain structures, composition and sequence of hydrophilic (ion-containing) and hydrophobic components, and membrane morphology.[19−21] Among them, acidity of ionic groups and membrane morphologies seem crucial, and they are correlated to each other.[22] The high acidity gives not only high concentration of mobile protons but also pronounced hydrophilic/hydrophobic phase separation.[23,24] The membrane morphology with well-connected hydrophilic channels results in facile diffusion of protons and water molecules, leading to high proton conductivity. Recent researches have revealed that block copolymer architecture[25−29] and introducing highly sulfonated hydrophilic moieties[30,31] are effective approaches for the purpose. The resulting ionomer membranes showed improved proton conductivity; however, the conductivity was still insufficient under low RH conditions.

Recently, we have synthesized a new series of multiblock sulfonated poly(arylene ether sulfone)s (B-SPESs) containing highly sulfonated hydrophilic component.[32] The postsulfonation reaction of the precursor polymers afforded highly sulfonated hydrophilic block. The B-SPES membranes showed more developed phase separation between hydrophobic and hydrophilic blocks than that of the random copolymer equivalents. Similar strategy was also reported for polyimide block copolymers by Li et al.[33] More recently, we have preliminarily reported advanced version of B-SPESs, multiblock sulfonated poly(arylene ether sulfone ketone)s (B-SPESKs), in which sulfone−ketone structure of hydrophobic blocks enabled complete sulfonation reaction.[34] The B-SPESK membranes with 1.62 mequiv/g of ion exchange capacity (IEC) showed comparable proton conductivity to Nafion at 20−90% RH and 80 °C. A fuel cell was successfully operated with the membrane at 30% and 53% RH, 100 °C. In this paper, we report detailed investigation on synthesis and properties of the B-SPESK membranes.

Experimental Section

Bis(4-fluorophenyl)sulfone (FPS) and 4,4′-dihydroxybenzophenone (DHBP) were purchased from TCI, Inc., and recrystallized from toluene. 9,9-Bis(4-hydroxyphenyl)fluorene (BHF) was purchased from TCI., Inc., and recrystallized from toluene/ethanol. Potassium carbonate, calcium carbonate, and toluene were purchased from Kanto Chemical Co. and used as received. *N,N*-Dimethylacetamide (DMAc, organic synthesis grade, 99%)

*Corresponding author: Tel +81 55 220 8707; e-mail miyatake@yamanashi.ac.jp. jp (K.M.); Tel +81 55 254 7091; e-mail m-watanabe@yamanashi.ac.jp (M.W.).

 Published on Web 02/18/2010

was purchased from Kanto Chemical Co. and dried over 4 Å molecular sieves prior to use. Nafion membranes were purchased from DuPont and were treated with hot 5 wt % H_2O_2 aqueous solution for 1 h and boiling 1 M H_2SO_4 aqueous solution for 1 h and washed with deionized water several times.

Hydroxy-terminated telechelic oligomers (**1a**), fluorine-terminated telechelic oligomers (**1b**), block copolymers (**2**), and sulfonated block copolymers (**3**) were synthesized as previously reported.[34] A 50 μm membrane was prepared by casting from DMAc solution. Characterizations of oligomers, polymers, and their membranes such as ^{1}H NMR, GPC, titration, scanning transmission electron microscopy (STEM), small-angle X-ray scattering (SAXS), water uptake, proton conductivity, and oxidative and hydrolytic stability were carried out according to the method previously reported.[34] For STEM observations, the membrane samples were stained with lead ions by ion exchange of the sulfonic acid groups in 0.5 M lead acetate aqueous solution, rinsed with deionized water, and dried in vacuum oven for 12 h. SAXS was measured for fully hydrated samples of **3**, random sulfonated poly(arylene ether sulfone) (SPES), and Nafion NRE membranes at room temperature. Density of dry **3** and Nafion membranes was measured by a pycnometer (Ultrapycnometer1000, Quantachrome Inc.) using helium as test gas at room temperature. Density at 80 °C was calibrated by use of the volume expansion coefficient of perfluoroalkyl polymer (PFA: 1.3×10^{-4} K^{-1}) and poly(ether sulfone) (PSF: 3.1×10^{-4} K^{-1}), since the coefficients of the sulfonated polymers were not available. The density of sulfonated block copolymer **3** membranes was found to be between 1.36 and 1.67 g/cm^3 depending on the IEC.

From the water uptake and density data, volumetric IEC (IEC$_v$, mequiv/cm^3) was calculated by the following equation

$$\mathrm{IEC_v} = \frac{\mathrm{IEC_w}}{\dfrac{1}{\rho_{\text{polymer at 80 °C}}} + \dfrac{\text{water uptake (\%)}}{100 \times \rho_{\text{water at 80 °C}}}} \quad (1)$$

where IEC$_w$ is the gravimetric IEC (mequiv/g) and ρ (g/cm^3) is the density.

From the conductivity and density data, proton diffusion coefficient (D_σ) was calculated using the Nernst−Einstein equation

$$D_\sigma = \frac{RT}{F^2}\frac{\sigma}{c(\mathrm{H^+})} \quad (2)$$

where R is gas constant, T is the absolute temperature (K), F is the Faraday constant, and $c(H^+)$ is the concentration of proton charge carrier (mol/L).

Tensile strength was measured by universal test machine (AGS-J 500N, Shimadzu) attached with a temperature and humidity controllable chamber (Bethel-3A, Toshin Kogyo). Stress vs strain curves were obtained for samples cut into a dumbbell shape (DIN-53504-S3, 35 mm × 6 mm (total) and 12 mm × 2 mm (test area)). The measurement was conducted at 93% RH and 85 °C at a stretching speed of 10 mm/min.

Hydrogen and oxygen permeability was measured with a gas permeation measurement apparatus (20XFYC, GTR-Tech Inc.), and concentration of the permeated gases was quantified with a gas chromatograph (GC, G2700T, Yanaco) with thermal conductivity detector. Argon and helium were used as carriers for the measurement of hydrogen and oxygen, respectively. Membranes were placed in the center of the permeation cell, and the test gas was introduced onto one side of the membrane at a flow rate of 20 mL/min. Carrier gas was introduced onto the other side of the membrane at the same flow rate and was analyzed by the GC. The same humidity conditions were applied to both test and carrier gases to ensure homogeneous wetting of the membrane samples. The membrane was equilibrated until stable permeation data were obtained. The gas permeability coefficient, Q (cm^3 (STD) cm cm^{-2} s^{-1} cmHg^{-1}), was calculated by the equation

$$Q = \frac{273}{T}\frac{1}{A}B\frac{1}{t}l\frac{1}{76 - P_{\text{water}}} \quad (3)$$

where T (K) is the absolute temperature, A (cm^2) is the permeation area, B (cm^3) is the volume of the test gas permeated through the membrane, t (s) is the sampling time, l (cm) is the thickness of the membrane, and P_{water} (cmHg) is the water vapor pressure.

Results and Discussion

Synthesis and Characterization of OH-Terminated Telechelic Oligomers (1a). The synthetic procedure of the OH-terminated telechelic oligomers is shown in Scheme 1. The monomer composition was set so that the degree of polymerization (Y) would be 4, 8, 12, or 16. The oligomerization reaction proceeded in DMAc under typical nucleophilic substitution conditions using potassium carbonate as a base to give **1a**. The oligomers **1a** were obtained as a white powder and characterized by ^{1}H NMR spectra and GPC analyses. Molecular weight distribution (M_w/M_n) ranged from 1.9 to 2.5 and was typical for polycondensation reaction (Supporting Information Figure S1). The experimental Y values calculated from M_n were 5.0, 8.6, 13.0, and 17.9 for Y = 4, 8, 12, and 16, respectively. These values were roughly consistent with the ones expected from the feed ratio of the comonomers. In the ^{1}H NMR spectrum of **1a**, protons attached to OH-terminated phenylene rings appeared at higher magnetic field than those attached to oxyphenylene rings due to the strong electron-donating nature of hydroxy groups. The Y values calculated from the integral ratio of these peaks were 5.9, 9.8, 11.6, and 15.5 for Y = 4, 8, 12, and 16, respectively. These values were similar to the above Y values obtained by the GPC data. For the succeeding block copolymerization, Y values obtained by NMR spectra were used to balance the stoichiometry.

Synthesis and Characterization of F-Terminated Telechelic Oligomers (1b). The synthetic procedure of F-terminated telechelic oligomers is also shown in Scheme 1. The monomer composition was set so that the degree of polymerization (X) would be 15, 30, or 60. The oligomerization conditions were similar to those for **1a**, except that excess calcium carbonate was effectively added to complete the oligomerization reaction without reverse polycondensation or main chain cleavages.[30,35] In order to confirm the chemical structure and degree of polymerization, controlled reaction was conducted, in which the products were isolated and characterized by ^{1}H NMR spectra. In the ^{1}H NMR spectra of **1b**, protons of F-terminated sulfonylphenylene rings appeared at lower magnetic field than those attached to the sulfonylphenyleneoxy rings due to the strong electron-withdrawing nature of the fluorine groups. In the case of **1b** (X = 15), for example, the experimental X value calculated from the integral ratio was 13.1 close to the targeted value. The oligomers **1b** were not isolated in the actual block copolymerization in order to simplify the synthetic procedure (oligomers **1a** were added to the reaction mixtures of **1b** for the block copolymerization).

Synthesis and Sulfonation of Multiblock Copolymers. Block copolymerization of the oligomers **1a** and **1b** was also carried out in the presence of excess calcium carbonate in order to avoid reverse polymerization or main chain cleavage. Short polymerization time for 3 h was enough to give a highly viscous mixture containing high molecular weight products. The copolymers **2** were obtained as white fibers,

Scheme 1. Synthesis of OH-Terminated Telechelic Oligomers (1a), F-Terminated Telechelic Oligomers (1b), Block Copolymers (2), and Sulfonated Block Copolymers (3)

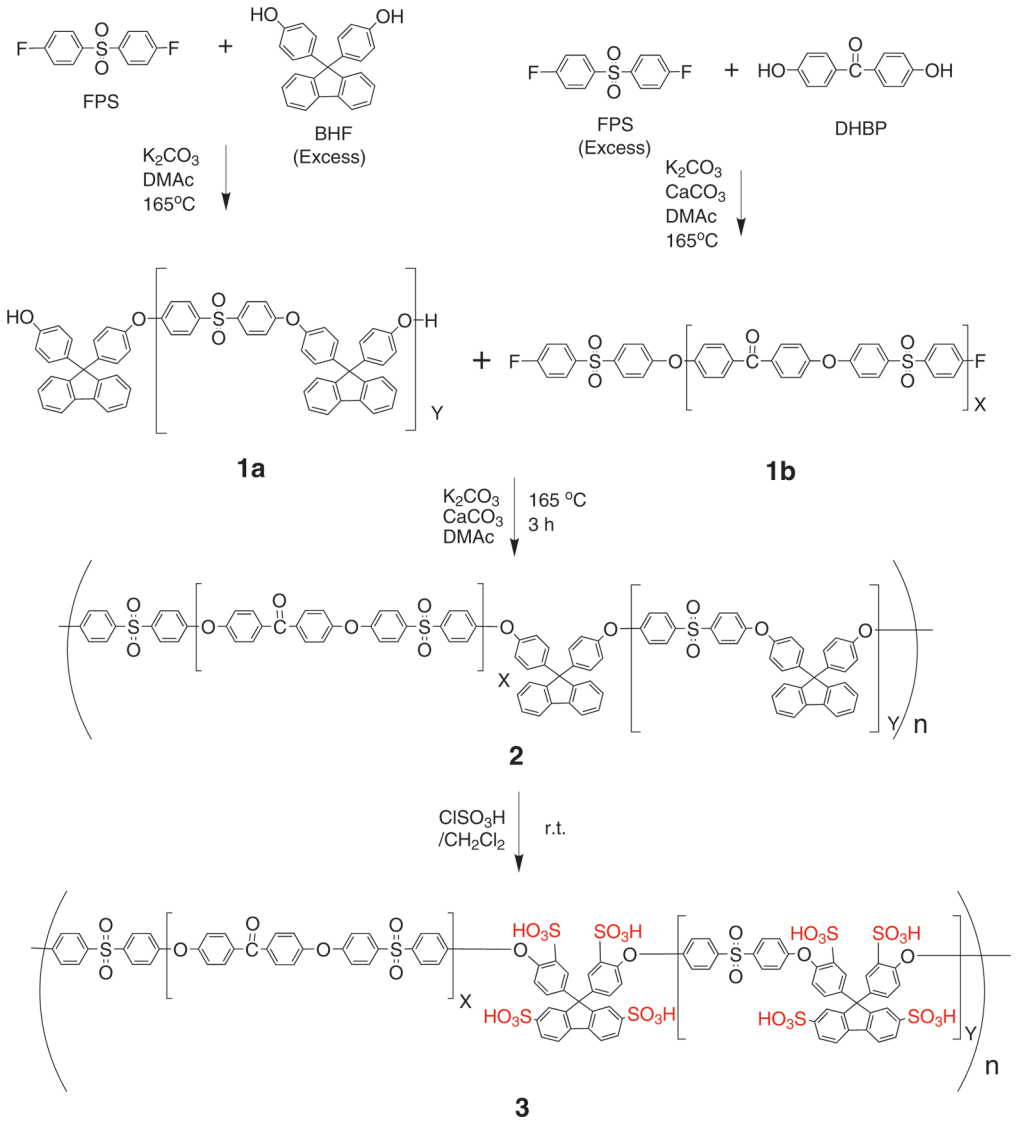

which were soluble in many organic solvents such as chloroform, DMF, DMSO, and DMAc. Comparison of the NMR spectra with those of the parent OH-terminated and F-terminated oligomers **1a** and **1b** revealed that the protons of OH- and F-substituted terminal phenylene groups disappeared in the obtained block copolymers, and the other peaks were consistent with those of the parent oligomers. GPC analyses showed unimodal elution curves with M_n > 57 kDa and M_w > 122 kDa (Figure S2). These results indicate the formation of multiblock copolymers. The *X* values in **2** were experimentally determined from the *Y* values of **1a** and M_n values of **2** and are summarized in Table 1. These experimental *X* values were nearly comparable to the ones expected from the feed comonomer composition.

Based on the experimental *X* and *Y* values, 5 excess equimolar chlorosulfonic acid was applied for the sulfonation reaction of **2**. The reaction proceeded well in dichloromethane solution at room temperature, and most of the product was precipitated out of the mixture within 1 h. The reaction, however, was continued for 24 h to ensure the complete sulfonation reaction. The sulfonated products **3** were isolated as white powders, which were soluble in DMSO and DMAc. In Figure S3a is shown the ^{1}H NMR spectrum of **3** (*X*60*Y*8) in Na^+ form. Comparison with those of the parent copolymers **2** revealed that the proton peaks assigned to the unsulfonated fluorenylidene biphenylene units (5−10) disappeared and the other aromatic rings (1−4, 1′, and 2′) were intact through the sulfonation reaction. Instead, new peaks assigned to the sulfonated fluorenylidene biphenylene groups appeared at 11−16. Absence of peaks 5−10 is indicative of complete sulfonation (100% of degree of sulfonation) on each phenylene ring of fluorenylidene biphenylene unit. GPC results did not show evidence of main chain degradation during the sulfonation reaction (Figure S2). Because of the electrostatic repulsion among sulfonic acid groups, the apparent molecular weight of **3** was larger than that of **2**. In our previous series of sulfonated multiblock poly(arylene ether sulfone)s, minor main chain degradation occurred at isopropylidene biphenylene (bisphenol A) moieties via the sulfonation reaction.[32] The copolymers **2**, in which bisphenol A groups were replaced with more robust benzophenone groups, were able to achieve completely sulfonated ionomers **3** without losing high molecular weight.

The ionomers **3** gave transparent and flexible films by solution casting. The gravimetric IEC (in mequiv/g) of the membranes were measured by back-titration and are

Table 1. Physical Properties of the Sulfonated Multiblock Copolymers 3 and Their Membranes

			volumetric IEC[b]			molecular weight (kDa)[c]			
						before sulfonation		after sulfonation	
expected *XY*	experimental *XY*	experimental IEC[a]	0% RH	80% RH	degree of sulfonation (%)	M_n	M_w	M_n	M_w
*X*15*Y*4	*X*12*Y*5	2.04	3.22	2.31	100	57	122	69	335
*X*30*Y*4	*X*25*Y*5	1.34	1.90	1.54	100	78	164	81	204
*X*15*Y*8	*X*14*Y*9	2.45	4.09	2.76	100	78	190	28	561
*X*30*Y*8	*X*25*Y*9	1.86	2.86	2.12	100	86	145	68	352
*X*60*Y*8	*X*51*Y*9	1.07	1.46	1.23	100	79	150	81	192
*X*30*Y*12	*X*25*Y*13	2.12	3.39	2.42	100	88	206	90	400
*X*60*Y*12	*X*53*Y*13	1.41	2.03	1.60	100	75	170	75	350
*X*30*Y*16	*X*23*Y*18	2.43	4.03	2.69	100	88	136	76	366
*X*60*Y*16	*X*56*Y*18	1.74	2.63	1.98	100	93	178	75	224
Nafion	N/A	0.91	1.83	1.48	N/A	N/A	N/A	N/A	N/A

[a] Obtained by back-titration (mequiv/g). [b] In mmol of sulfonic acid per total volume of water and polymer (calculated by eq 1, mequiv/cm^3). [c] Determined by GPC.

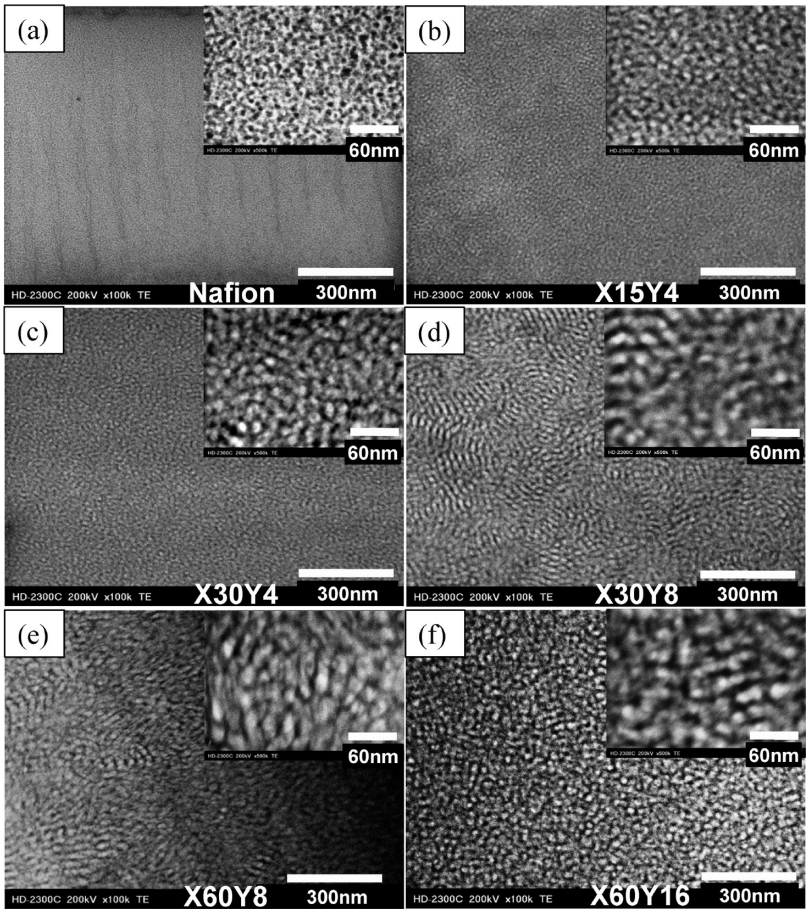

Figure 1. STEM images of lead ion-exchanged (a) Nafion NRE 212, (b) **3** (*X*15*Y*4; IEC = 2.04 mequiv/g), (c) **3** (*X*30*Y*4; IEC = 1.34 mequiv/g), (d) **3** (*X*30*Y*8; IEC = 1.86 mequiv/g), (e) **3** (*X*60*Y*8; IEC = 1.07 mequiv/g), and (f) **3** (*X*60*Y*16; IEC = 1.74 mequiv/g) membranes. Magnification of inset pictures is 500K (60 nm scale), and that of large pictures is 100K (300 nm scale).

included in Table 1. The IEC values ranged from 1.07 to 2.45 mequiv/g, depending on the number of repeating unit in hydrophobic (*X*) and hydrophilic (*Y*) blocks.

Morphologies of 3 Membranes. Morphologies of **3** membranes were investigated by STEM and SAXS analyses. Figure 1 shows cross-sectional STEM images of lead-ion exchanged samples. The images were taken at transmission electron mode, in which black domain represents lead-ion exchanged sulfonic acid groups (hydrophilic aggregates). Nafion NRE 212 membrane showed distinct and well-developed hydrophilic aggregates with ca. 4−5 nm in diameter (Figure 1a), which are recognized to account for its high proton conductivity. In contrast, hydrophilic aggregates were larger for **3** membranes and dependent on the block length (Figure 1b−f). Membranes **3** showed more enhanced phase separation than our previous random or block copolymers,[32,36] which was presumably due to higher concentration of sulfonic acid groups in the hydrophilic blocks. As observed in the lower magnification view, the hydrophilic domains were well-interconnected at least in micrometer scale. It is reasonable that the hydrophilic aggregates became larger as increasing the IEC ((c) *X*30*Y*4, 1.34 mequiv/g → (d) *X*30*Y*8, 1.86 mequiv/g and (e) *X*60*Y*8, 1.07 mequiv/g → (f) *X*60*Y*16, 1.74 mequiv/g) due to increased concentration of sulfonic acid groups. The effect of block length on the morphology is noticeable. Comparison among the three

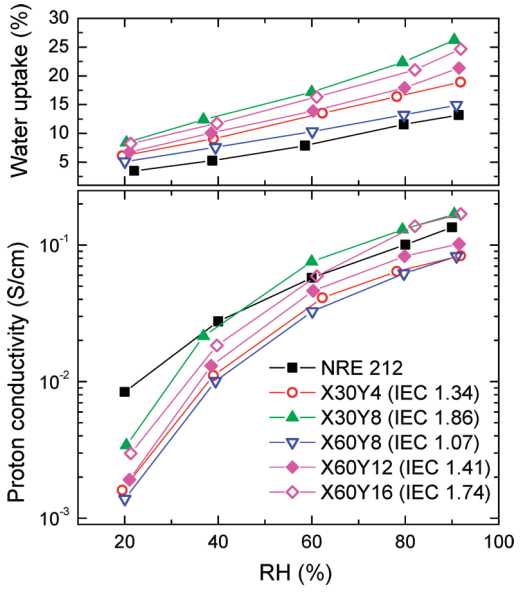

Figure 2. Water uptake and proton conductivity of **3** membranes with low IEC (< 2.0 mequiv/g) **3** at 80 °C as a function of RH.

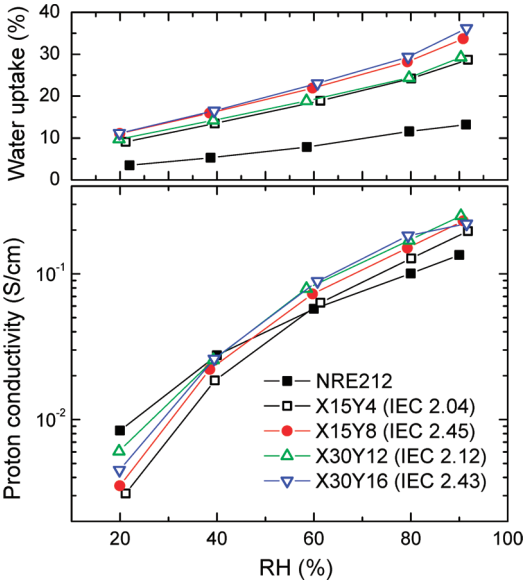

Figure 3. Water uptake and proton conductivity of **3** membranes with high IEC (> 2.0 mequiv/g) at 80 °C as a function of RH.

membranes with the same *X*/*Y* ratio revealed that the clusters became larger as increasing the block length ((b) *X*15*Y*4, 2.04 mequiv/g → (d) *X*30*Y*8, 1.86 mequiv/g → (f) *X*60*Y*16, 1.74 mequiv/g) despite that the IEC values were slightly decreasing. These results led to the conclusion that both IEC and block length are crucial factors in determining the membrane morphology while the latter is more influential.

Since STEM observation was carried out for dry samples under vacuum, SAXS measurements were applied to analyze hydrophilic clusters (aggregates) in hydrated samples. As reported in our previous communication,[34] **3** (*X*30*Y*8) and **3** (*X*60*Y*8) showed ca. 11 nm of Bragg distance, which is considered as the distance between ionic clusters and larger than that (5 nm) of Nafion membrane. Additional data were taken for **3** (*X*15*Y*4) and **3** (*X*30*Y*4) membranes under the same conditions to obtain the similar results. The results imply that, unlike the dry conditions, their IEC and block length were not major factors in determining the morphology under fully hydrated conditions. These morphological considerations will be further discussed below with water uptake and proton conductivity properties.

Water Uptake and Proton Conductivity of 3 Membranes. Figure 2 (IEC = 1.34−1.86 mequiv/g) and Figure 3 (IEC > 2.04 mequiv/g) show water uptake and proton conductivity of **3** membranes as a function of RH at 80 °C. As a reference, Nafion NRE212 showed 13% water uptake at 90% RH, which was much lower than 50% water uptake in water at 100 °C as suggested by DuPont.[37] As expected, higher IEC membranes absorbed more water due to the increased hydrophilicity. The highest water uptake was 36% at 92% RH for the highest IEC membrane (2.43 mequiv/g), which was ~3 times higher than that of Nafion NRE membrane. Unlike the previous series of our block copolymers[32] and other reports,[27,33] in which the longer block length induced higher water uptake, the block length was less likely to affect the water uptake for **3** membranes; compare *X*30*Y*8 and *X*60*Y*16 in Figure 2 or *X*15*Y*8 and *X*30*Y*16 in Figure 3. A possible explanation for this behavior would be that **3** contains polar and rigid groups in the hydrophobic blocks; however, further analyses with different block length and different hydrophobic component would be needed to obtain decisive ideas.

Dimensional stability of selected membranes was also tested at room temperature by use of water swelling ratio, which was defined as increased length or thickness of membranes at swelling divided by the dimension of dry samples. SPESK membranes showed anisotropic swelling behavior with larger dimensional change in *through-plane* direction than in *in-plane* direction. For example, *X*60*Y*8 (IEC = 1.07 mequiv/g) showed 6 and 8% swelling in *x*- and *y*-direction, whereas its *z*-direction swelling was 30%. Other samples such as *X*30*Y*4 and *X*60*Y*16 showed a similar tendency, which was in good accordance with the other report.[27]

Similar to the water uptake, the higher IEC membranes showed higher proton conductivity at all RHs investigated. Compared to our previous random and block copolymers with similar chemical structure and IEC values,[32,36] **3** membranes showed higher proton conductivity particularly at low RH. For example, *X*30*Y*8 with IEC = 1.86 mequiv/g showed 0.13 and 0.03 S/cm at 80% and 40% RH, whereas NRE212 showed 0.10 and 0.03 S/cm at 80% and 40% RH, respectively. The **3** membranes with IEC > 1.86 mequiv/g showed comparable or higher proton conductivity than that of Nafion NRE 212 membrane at >40% RH. The high proton conductivity is attributable to the well-connected and large ionic clusters as confirmed in STEM and SAXS analyses. The effect of block length is consistent with the morphology in the STEM images. The **3** (*X*60*Y*8, IEC = 1.07 mequiv/g) having longer blocks showed similar proton conductivity to that of **3** (*X*30*Y*4, IEC = 1.34 mequiv/g) in spite of the former's lower IEC and water uptake. A similar tendency was observed for higher IEC membranes; compare **3** (*X*30*Y*8, IEC = 1.86 mequiv/g) and **3** (*X*15*Y*4, IEC = 2.04 mequiv/g). For the practical fuel cell applications, we have concluded that the best balanced membrane would be **3** (*X*30*Y*8, IEC = 1.86 mequiv/g) showing high proton conductivity at wide range of humidity for its relatively low IEC and water uptake.

For the detailed comparison of the proton conductivity among the membranes at different RH, volumetric IEC (IEC_v, mequiv/cm^3)[38] that is defined as molar concentration of sulfonic acid groups per unit volume containing absorbed water was calculated. The IEC_v is plotted as a function of RH in Figure S4. The IEC_v values became lower as increasing

RH due to increased water volume within the polymer matrix. Nafion NRE and **3** (*X*30*Y*4) membranes showed approximately the same IEC_v values at a wide range of humidity, since the differences in their gravimetric IEC were counterbalanced by the differences in their density (2.01 g/cm^3 for Nafion and 1.42 g/cm^3 for **3** (*X*30*Y*4)) and the two membranes shared a similar dependency of the water uptake upon humidity.

In Figure 4 is plotted proton diffusion coefficient (D_σ) as a function of IEC_v. Compared to **3** membranes, Nafion NRE showed higher D_σ for its lower IEC_v. D_σ of Nafion ranged from 2.99×10^{-5} to 1.57×10^{-6} cm^2/s, designated as Nafion region in Figure 4, and the region is much narrower than that of the **3** membranes. The results imply that D_σ of Nafion is less dependent on the humidity. At 90% RH, which corresponds to the uppermost plot for each membrane sample, IEC_v higher than 1.9 mequiv/cm^3 was needed for the **3** membranes in order to have comparable D_σ to that of Nafion. At >40% RH, the lower D_σ of **3** membranes could be compensated by the higher IEC_v (or proton concentration). However, this was not the case at 20% RH since the differences in D_σ was too large to be compensated by IEC_v.

A general trend of the dependency of D_σ on the block length was obtained. At low IEC_v, *X*60*Y*8 showed higher D_σ than that of *X*30*Y*4. *X*60*Y*16 also showed higher or similar D_σ than that of *X*30*Y*8 and *X*15*Y*4 in spite of the former's lower IEC_v. These results are consistent with the fact that **3** membranes having longer block length showed higher proton conductivity. In addition, the D_σ values obtained for **3** membranes were much higher than those of our previous random copolymer membranes.[21] The results are not contradictory to the above-mentioned morphological data and validate our strategy of multiblock copolymers with highly sulfonated hydrophilic block for highly proton conductive ionomer membranes.

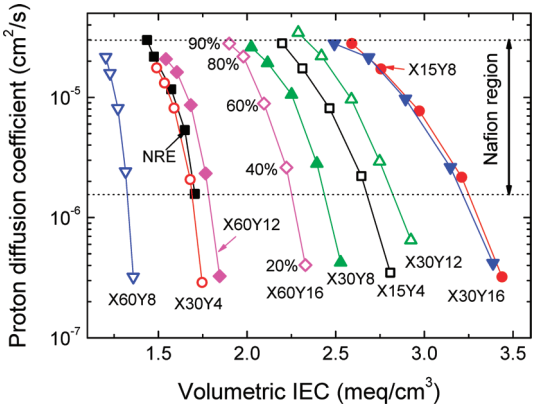

Figure 4. Proton diffusion coefficient of **3** and Nafion NRE212 membranes as a function of volumetric IEC_v at 80 °C.

Oxidative and Hydrolytic Stability of 3 Membranes. Oxidative and hydrolytic stability of **3** membranes was investigated under accelerated testing conditions in Fenton's reagent and hot water, respectively. Weight residue and molecular weight were analyzed before and after each stability test and are summarized in Table 2.

The Fenton test at 80 °C for 1 h dissolved most of **3** membranes with IEC > 2.0 mequiv/g. The **3** membranes with IEC < 2.0 mequiv/g showed residue and the residual weight increased as decreasing IEC. The molecular weight of the residues evaluated by GPC was lower than 30% of the original molecular weight, indicating that the ionomers dissolved with oxidative degradation. The slower degradation for lower IEC membranes is reasonable due to the lower water uptake and accordingly lower diffusion of peroxide and the derived radical species. Compared to our previous random copolymers,[36] **3** membranes were somewhat less stable to oxidation. This is probably because water molecules diffuse faster in **3** membranes as well as protons. It was suggested in the sulfonated poly(arylene ether sulfone)s that oxidative degradation is likely to occur at phenylene carbons *ortho* to the ether bonds (1 and 3 in Figure S3a) by the attack of hydroxyl radicals due to their high electron density.[39,40] The *ortho* carbons in the ionomers **3** are deactivated to such oxidative attack by strong electron-withdrawing sulfone and ketone groups. However, our results suggest that the diffusion of oxidative species is more crucial in the oxidative stability. For the practical fuel cell applications, oxidative stability of ionomer membranes is correlated with gas permeability, which will be discussed below.

The **3** membranes were stable to hydrolysis. The weight losses were much less than the oxidative weight losses, and the membranes with IEC < 2.0 mequiv/g did not show any losses in weight and molecular weight after the hydrolytic test. The higher IEC membranes dissolved into water to a certain degree; however, the recovered samples by evaporation of water retained their original molecular weight. The results indicate that **3** membranes do not degrade under these severe hydrolytic conditions, similar to our previous random copolymers.[36] Long-term stability was also tested in boiling water (100 °C) for 1000 h for two samples (*X*30*Y*8 and *X*60*Y*8). Both membranes did not show detectable changes in weight, molecular weight, IEC, and ^{1}H NMR spectra (Figure S3b).

Mechanical Properties of 3 Membranes. Elongation of **3** membranes was measured at 93% RH and 85 °C by a universal testing instrument. The mechanical properties were highly affected by IEC as appeared in stress vs strain curves (Figure 5 and Table 3). The block length had also some impact on the mechanical properties with the general trend

Table 2. Oxidative and Hydrolytic Stability of 3 Membranes

		after oxidative stability test[b]		after hydrolytic stability test[c]	
expected *XY*	IEC[a]	weight (%)[d]	residual molecular weight (%)[e]	weight (%)[d]	residual molecular weight (%)[e]
*X*15*Y*4	2.04	0	N/A	70	100
*X*30*Y*4	1.34	53	28	100	100
*X*15*Y*8	2.45	0	N/A	28	100
*X*30*Y*8	1.86	33	26	100	100
*X*60*Y*8	1.07	49	25	100	100
*X*30*Y*12	2.12	8	11	59	100
*X*60*Y*12	1.41	45	18	100	100
*X*30*Y*16	2.43	0	N/A	0	100
*X*60*Y*16	1.74	19	21	100	100

[a] In mequiv/g. [b] In Fenton's reagent (3% H_2O_2 containing 2 ppm $FeSO_4$) at 80 °C for 1 h. [c] Accelerated hydrolytic test in 140 °C water for 24 h. [d] Residual weight percent after the test. [e] Residual molecular weight percent by GPC.

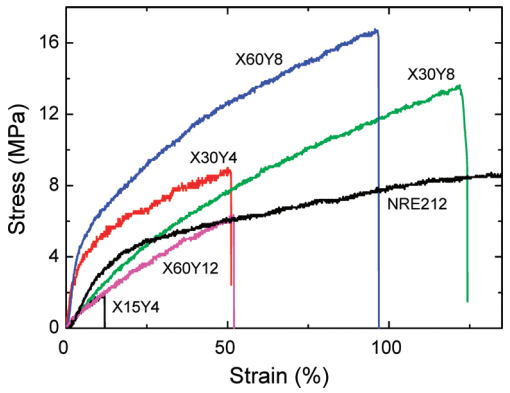

Figure 5. Stress vs strain curves of **3** membranes at 85 °C and 93% RH.

Table 3. Results of Elongation test of 3 Membranes at 85 °C and 93% RH

expected *XY*	strain (%)	maximum stress at break point (MPa)	Young's modulus (MPa)
*X*15*Y*4	12	1.9	16
*X*30*Y*4	51	8.9	139
*X*30*Y*8	124	13.6	22
*X*30*Y*12	20	2.6	16
*X*30*Y*16	23	1.4	7
*X*60*Y*8	97	16.7	125
*X*60*Y*12	52	6.3	16
*X*60*Y*16	27	3.6	18
NRE212	350	15.0	31

of lower Young's modulus for longer block length membranes. For example, *X*60*Y*12 and *X*60*Y*16 membranes showed lower stress at break point and lower Young's modulus than those of the shorter block length equivalents with similar IEC, *X*30*Y*4, and *X*30*Y*8, respectively. Compared to our previous random and block ionomer membranes, Young's moduli were lower for the **3** membranes.[21,32] The results would be reasonable taking higher water absorbability of **3** membranes into account. The developed hydrophilic aggregates in **3** membranes segregate hydrophobic blocks and consequently cause weaker physical interactions between hydrophobic blocks and lower mechanical strength of the membranes. In addition, **3** membranes did not show any peaks after initial elongation (stress relaxation), which was often observed in the random or other block copolymer membranes. Since this behavior is regarded as onset of disentanglement of bundles in the hydrophobic components, the results support the idea that the hydrophobic interaction is weak in the **3** membranes. It should be noticed, however, that Young's modulus of **3** membranes with IEC < 2.0 mequiv/g was still comparable to or higher than that of Nafion membrane, which showed very large elongation (350%) with 15 MPa of the stress at break point.

Hydrogen and Oxygen Permeability of 3 Membranes. Hydrogen and oxygen permeability of **3** (*X*30*Y*4), (*X*30*Y*8), (*X*60*Y*8), (*X*60*Y*16), and Nafion membranes were measured under dry conditions. The permeability coefficient is plotted as a function of temperature in Figure 6. The **3** membranes showed much lower hydrogen and oxygen permeability as well as lower activation energy than those of Nafion. The apparent activation energy of the gas permeability of Nafion was $E_a(H_2) = 38$ and $E_a(O_2) = 52$ kJ/mol, and that of **3** was $E_a(H_2) = 15-17$ and $E_a(O_2) = 17-20$ kJ/mol, which is comparable to those of our previous random copolymers.[36] The differences in the gas permeability between **3** and Nafion, therefore, were much more pronounced at higher temperature. For example, O_2 permeability coefficient of

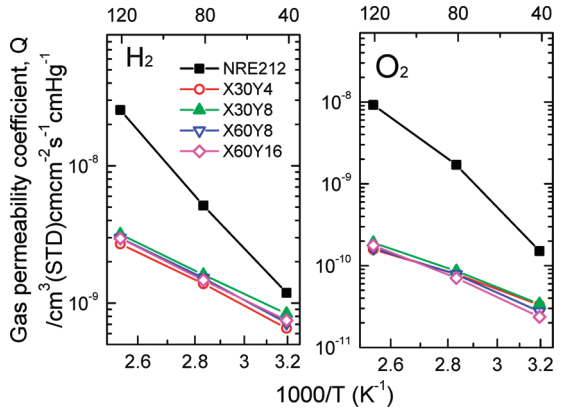

Figure 6. Temperature dependence of hydrogen and oxygen permeability coefficient of **3** (*X*30*Y*4), (*X*30*Y*8), (*X*60*Y*8), (*X*60*Y*16), and Nafion NRE212 membranes under dry conditions.

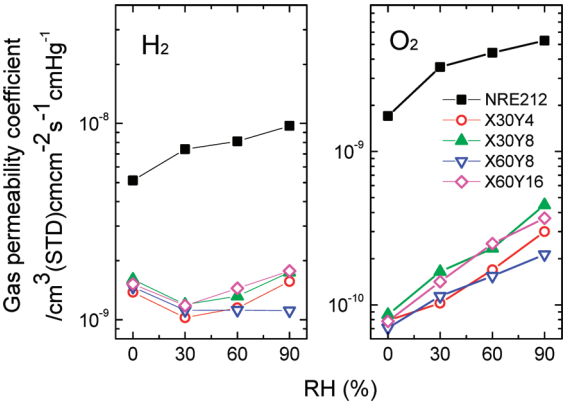

Figure 7. Humidity dependence of hydrogen and oxygen permeability coefficient of **3** (*X*30*Y*4), (*X*30*Y*8), (*X*60*Y*8), (*X*60*Y*16), and Nafion NRE212 membranes at 80 °C.

Nafion was 10^{-8} cm^3 (STD) cm cm^{-2} s^{-1} $cmHg^{-1}$ while that of **3** membranes was less than 2×10^{-10} cm^3 (STD) cm cm^{-2} s^{-1} $cmHg^{-1}$. The gas permeability of **3** membranes seemed independent of their IEC and block length. The results are rather surprising taking into account our previous results that hydrophobic component had a significant impact on gas permeability.[21] Since gas permeability under dry conditions is generally related to the free volume of membranes, such independency of the gas permeability on the concentration of sulfonic acid groups and block structure may imply that there exists a trade-off relationship between IEC and block structure to result in similar free volume in **3** membranes.

Figure 7 shows hydrogen and oxygen permeability under humidified conditions at 80 °C. At any humidity, the **3** membranes showed much lower gas permeability than Nafion while humidity dependence of the permeability was different for hydrogen and oxygen. In the case of hydrogen, the permeability of the **3** membranes decreased slightly with humidification (up to 30% RH) and then increased with further humidification. The behavior of hydrogen permeability was previously reported in the literature, and it was claimed that determining factor for the gas permeation changed with the amount of absorbed water.[41] When membranes are contacted with water vapor, water molecules are absorbed by sulfonic acid groups, which would decrease free volume and gas permeation of membranes. The role of hydrophilic component on gas permeation is not significant at low RH since hydrophilic channel would be under development. With further humidification, the membranes

absorb more water molecules and begin to develop hydrophilic clusters and their connectivity. Then, the contribution from the hydrophilic domains becomes significant to increase the total gas permeability of membranes. At higher RH, hydrophilic domains seem to dominate hydrogen permeation. It would be reasonable that higher IEC membrane, **3** (*X*60*Y*16) (1.74 mequiv/g), showed higher dependence of the gas permeability on humidity than the lower IEC membrane, **3** (*X*60*Y*8) (1.07 mequiv/g), due to the former's higher water absorbability. The inverted-volcano-type behavior of the gas permeability on the humidity was not observed for the Nafion membrane probably due to its highly developed water channels even at low RH.

Contrary to hydrogen permeability, oxygen permeability of **3** membranes increased from the initial stage of humidification, which was more similar to the behavior of Nafion membrane. The behavior was peculiar to the block copolymer membranes and was not observed for the random copolymer membranes.[36] The results may imply that hydrophilic domains are also influential in the oxygen permeation at low RH. Differences in the solubility of each gas in water containing hydrophilic clusters would be accountable, which need further investigation.

Conclusions

A series of sulfonated poly(arylene ether sulfone ketone) (SPESK) multiblock copolymers (**3**) having highly sulfonated hydrophilic blocks were successfully synthesized, and the degree of sulfonation reached nearly 100%. These novel block copolymer membranes showed highly developed phase separation under both dry and fully hydrated conditions. The **3** membranes showed much higher proton conductivity than that of our previous random and block copolymers at wide range of humidity. Longer block length seems effective in increasing proton diffusion coefficient, which coincide with the morphological observations. High mechanical strength as well as hydrolytic stability was maintained at high temperature. Very low hydrogen and oxygen permeability was also confirmed. The best balanced membrane was **3** (*X*30*Y*8) with high proton conductivity (0.13 and 0.03 S/cm at 80% and 40% RH, 80 °C) and mechanical stability for its relatively low IEC (1.86 mequiv/g) and water uptake. The **3** (*X*30*Y*8) membrane was hydrolytically stable in boiling water for 1000 h. Oxidative stability was mediocre; however, low gas permeability would compensate for the chemical stability. In a separate report, we will report detailed analyses of fuel cell performance with this new ionomer material as membranes and/or electrode binders.

Acknowledgment. This work was partly supported by the New Energy and Industrial Technology Development Organization (NEDO) through the HiPer-FC Project, and the Ministry of Education, Culture, Sports, Science and Technology (MEXT) Japan through a Grant-in-Aid for Scientific Research (20350086).

Supporting Information Available: ^{1}H NMR spectra and GPC profiles of oligomers and polymers. This material is available free of charge via the Internet at http://pubs.acs.org.

References and Notes

(1) Rozière, J.; Jones, D. J. *Annu. Rev. Mater. Res.* **2003**, *33*, 503–555.
(2) Lakshmanan, B.; Huang, W.; Olmeijer, D.; Weidner, J. W. *Electrochem. Solid-State Lett.* **2003**, *6*, A282–A285.
(3) Mathias, M. F.; Makharia, R.; Gasteiger, H. A.; Conley, J. J.; Fuller, T. J.; Gittleman, C. J.; Kocha, S. S.; Miller, D. P.; Mittelsteadt, C. K.; Xie, T.; Yan, S. G.; Yu, P. T. *Interface* **2005**, *14*, 24.
(4) Wang, F.; Hickner, M.; Kim, Y. S.; Zawodzinski, T. A.; McGrath, J. E. *J. Membr. Sci.* **2002**, *197*, 231–242.
(5) Chikashige, Y.; Chikyu, Y.; Miyatake, K.; Watanabe, M. *Macromolecules* **2005**, *38*, 7121–7126.
(6) Xing, P.; Robertson, G. P.; Guiver, M. D.; Mikhailenko, S. D.; Wang, K.; Kaliaguine, S. *J. Membr. Sci.* **2004**, *229*, 95–106.
(7) Gil, M.; Ji, X.; Li, X.; Na, H.; Hampsey, J. E.; Lu, Y. *J. Membr. Sci.* **2004**, *234*, 75–81.
(8) Shang, X.; Tian, S.; Kong, L.; Meng, Y. *J. Membr. Sci.* **2005**, *266*, 94–101.
(9) Schuster, M.; Kreuer, K.-D.; Andersen, H. T.; Maier, J. *Macromolecules* **2007**, *40*, 598–607.
(10) Bai, Z.; Dang, T. D. *Macromol. Rapid Commun.* **2006**, *27*, 1271–1277.
(11) Miyatake, K.; Zhou, H.; Matsuo, T.; Uchida, H.; Watanabe, M. *Macromolecules* **2004**, *37*, 4961–4966.
(12) Yin, Y.; Suto, Y.; Sakabe, T.; Chen, S.; Hayashi, S.; Mishima, T.; Yamada, O.; Tanaka, K.; Kita, H.; Okamoto, K.-i. *Macromolecules* **2006**, *39*, 1189–1198.
(13) Gao, Y.; Robertson, G. P.; Kim, D.-S.; Guiver, M. D.; Mikhailenko, S. D.; Li, X.; Kaliaguine, S. *Macromolecules* **2007**, *40*, 1512–1520.
(14) Wainright, J. S.; Wang, J.-T.; Weng, D.; Savinell, R. F.; Litt, M. *J. Electrochem. Soc.* **1995**, *142*, L121.
(15) Glipa, X.; El Haddad, M.; Jones, D. J.; Rozière, J. *Solid State Ionics* **1997**, *97*, 323–331.
(16) Kobayashi, T.; Rikukawa, M.; Sanui, K.; Ogata, N. *Solid State Ionics* **1998**, *106*, 219–225.
(17) Fujimoto, C. H.; Hickner, M. A.; Cornelius, C. J.; Loy, D. A. *Macromolecules* **2005**, *38*, 5010–5016.
(18) Fuel Cell Program's Multi-Year Research, Development, and Demonstration Plan. http://www1.eere.energy.gov/hydrogenandfuelcells/fuelcells/fc_challenges.html.
(19) Rikukawa, M.; Sanui, K. *Prog. Polym. Sci.* **2000**, *25*, 1463–1502.
(20) Ghassemi, H.; McGrath, J. E.; Zawodzinski, T. A. *Polymer* **2006**, *47*, 4132–4139.
(21) Bae, B.; Miyatake, K.; Watanabe, M. *Macromolecules* **2009**, *42*, 1873–1880.
(22) Kreuer, K. D. *J. Membr. Sci.* **2001**, *185*, 29–39.
(23) Miyatake, K.; Shimura, T.; Mikami, T.; Watanabe, M. *Chem. Commun.* **2009**, 6403–6405.
(24) Yoshimura, K.; Iwasaki, K. *Macromolecules* **2009**, *42*, 9302–9306.
(25) Nakano, T.; Nagaoka, S.; Kawakami, H. *Polym. Adv. Technol.* **2005**, *16*, 753–757.
(26) Schöberger, F.; Kerres, J. *J. Polym. Sci., Part A: Polym. Chem.* **2007**, *45*, 5237–5255.
(27) Lee, H.-S.; Roy, A.; Lane, O.; Dunn, S.; McGrath, J. E. *Polymer* **2008**, *49*, 715–723.
(28) Goto, K.; Rozhanskii, I.; Yamakawa, Y.; Otsuki, T.; Naito, Y. *Polym. J.* **2009**, *41*, 95–104.
(29) Roy, A.; Yu, X.; Dunn, S.; McGrath, J. E. *J. Membr. Sci.* **2009**, *327*, 118–124.
(30) Matsumura, S.; Hlil, A. R.; Lepiller, C.; Gaudet, J.; Guay, D.; Shi, Z.; Holdcroft, S.; Hay, A. S. *Macromolecules* **2008**, *41*, 281–284.
(31) Matsumura, S.; Hlil, A. R.; Hay, A. S. *J. Polym. Sci., Part A: Polym. Chem.* **2008**, *46*, 6365–6375.
(32) Bae, B.; Miyatake, K.; Watanabe, M. *ACS Appl. Mater. Interfaces* **2009**, *1*, 1279.
(33) Li, N.; Liu, J.; Cui, Z.; Zhang, S.; Xing, W. *Polymer* **2009**, *50*, 4505–4511.
(34) Bae, B.; Yoda, T.; Miyatake, K.; Uchida, H.; Watanabe, M. *Angew. Chem., Int. Ed.* **2010**, *49*, 317–320.
(35) Martínez, C. A.; Hay, A. S. *J. Polym. Sci., Part A: Polym. Chem.* **1997**, *35*, 1781–1798.
(36) Bae, B.; Miyatake, K.; Watanabe, M. *J. Membr. Sci.* **2008**, *310*, 110–118.
(37) Data sheet of Nafion membranes (dispersion-cast). http://www2.dupont.com/FuelCells/en_US/assets/downloads/dfc201.pdf.
(38) Einsla, M. L.; Kim, Y. S.; Hawley, M.; Lee, H.-S.; McGrath, J. E.; Liu, B.; Guiver, M. D.; Pivovar, B. S. *Chem. Mater.* **2008**, *20*, 5636–5642.
(39) Hubner, G.; Roduner, E. *J. Mater. Chem.* **1999**, *9*, 409–418.
(40) Zhang, L.; Mukerjee, S. *J. Electrochem. Soc.* **2006**, *153*, A1062–A1072.
(41) Piroux, F.; Espuche, E.; Mercier, R. *J. Membr. Sci.* **2004**, *232*, 115–122.